The impact of modelling and prediction errors on the performance of optimally controlled multi-DOF wave energy converters

A.J. Hillis * **J. Yardley** * **A.R. Plummer** * **J. Chapman** **

* *University of Bath, Department of Mechanical Engineering, Bath BA27AY, UK (e-mail: a.j.hillis@bath.ac.uk, a.r.plummer@bath.ac.uk).*
** *Marine Power Systems Ltd, Ethos Building, Kings Road, Swansea, SA1 8AS (e-mail: contact@marinepowersystems.co.uk).*

Abstract: A well-conceived real-time control strategy can greatly increase the captured power for a wave energy converter (WEC). Optimal strategies rely on a dynamic model of the WEC and prediction of the wave excitation force several seconds into the future. Both the modelling and prediction processes are subject to errors. This paper investigates the impact of these errors on the performance of a multi-DOF submerged point absorber WEC. A state-space model of the system in its nominal position is derived and used by the control strategy. This idealised system is tested in multiple numerically generated irregular sea states with perfect estimation and prediction of the excitation force assumed. An optimally tuned passively damped system is used as a performance benchmark. The idealised system under optimal control is capable of more than doubling the captured power compared to the passively damped system. The control strategy is then applied to a full kinematic model of the WEC in the WEC-Sim environment. Real-time estimation and prediction of the excitation forces and constraints on motion and control force are also included. Under these more realistic conditions, the power gain is a more modest 68% at best across the tested sea states, and for one tested sea state there is no power gain compared to the passive system. Overall the gains are still significant and demonstrate the potential benefits of such control strategies for application to multi-DOF WECs, though more robust alternatives may be preferable.

Keywords: Wave energy converter, model predictive control, real-time estimation, prediction.

1. INTRODUCTION

The control system is key to enabling wave energy converters (WECs) to become economically viable by maximising energy capture in variable sea states. Many control strategies have been proposed to achieve a practically implementable optimal or sub-optimal power maximising objective. This study is concerned with the application of model-based optimal control strategies and uses a Model Predictive Control (MPC) formulation. Example WEC applications of MPC can be found in Hals et al. (2010), Cretel et al. (2011) and Richter et al. (2013) and many variants have been proposed.

Many simulation studies on this topic use a simplified buoy WEC constrained to move only in heave. The hydrodynamics are approximated by Boundary Element Method (BEM) solutions and embedded within the idealised model around which the MPC is formulated. The controller performance is then established by application to a system with identical dynamics, thus the assumption is that there is no model mismatch. MPC and other optimal strategies also require future knowledge of the wave excitation force. The common assumption is that this knowledge is readily available and many studies will assume perfect prediction over any control horizon. In practice the excitation force must be estimated (again a model-based procedure) and then forecast on-line based upon measurements and historical data. Errors will inevitably be introduced but there are relatively few studies that investigate the more realistic deployable situations. The focus here is not on the improvement of the control, but rather to test the effects on system performance of removing common assumptions made in other studies.

The sensitivity of an MPC control strategy to model mismatch in the hydrodynamics (mass, damping and stiffness) has been studied in O'Sullivan (2017) with application to a simulated heaving buoy. The most significant performance degradation was found to be related to mismatch in the hydrodynamic stiffness model. A more generic study of closed-loop sensitivity to hydrodynamic model mismatch was conducted in Ringwood et al. (2019). The hydrodynamic added mass, radiation damping and hydrostatic stiffness parameters are varied from those fixed in the controller model. Two common control structures are investigated - approximate conjugate control (ACC) and approximate optimal velocity tracking control (AVT). These are applied to a simplified heaving buoy and the sensitivity of power absorption to parameter variations is established. It is found that ACC is sensitive to inertial and stiffness errors while the AVT is less so due to the robust nature of the tracking loop. In both studies perfect knowledge of the future wave exci-

tation over the prediction horizon was assumed, though errors here will inevitably impact on the overall system performance.

Here we study the effects of prediction errors and model mismatch by applying an MPC law to a specific multi-DOF WEC, known as WaveSub, in two different situations. Firstly, the commonly studied ideal situation assuming perfect prediction over any horizon and no mismatch between the controller model and the controlled system. Secondly, a WEC-Sim (Yu et al. (2014)) simulation which includes on-line estimation and prediction of the excitation force. The model includes full kinematic constraints, yielding a system which is nonlinear due to large motions causing significant variation of the mechanical stiffness matrix.

The remainder of this paper is organised as follows. An overview of the WaveSub WEC is provided in section 2. Section 3 provides a description of the linearised equivalent model for use in the controller. The MPC law is described in section 4 and a method for wave force estimation and forecasting is given in section 5. Simulation results for the idealised and WEC-Sim cases are provided in sections 6 and 7 and conclusions are provided in section 8.

2. OVERVIEW OF THE WAVESUB WEC

WaveSub is under development by Marine Power Systems Ltd (MPS). It is a submerged point absorber with a unique multi-tether configuration and variable geometry which can be tuned to the prevailing sea state. A float moves with the waves and reacts against a moored base. The tethers pull on rotational drums which are attached to a PTO. Figure 1 shows an image of the simplified geometry used for simulation in the WEC-Sim package. The float has diameter 12m and the reactor length is 50m.

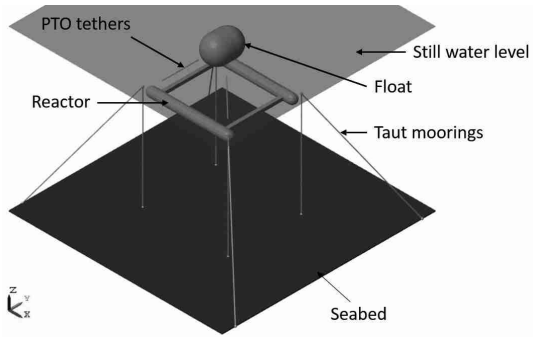

Fig. 1. Simplified geometry and mooring in WEC-Sim

3. LINEARISED DYNAMIC SYSTEM MODEL

The MPC formulation requires a linearised approximation to the WEC and PTO systems. For simplicity we assume the reactor to be fixed as a taut mooring system is used. Therefore, the WEC dynamics can be represented by the state-space system

$$\begin{aligned}\dot{\mathbf{x}}^+(t) = \begin{bmatrix}\dot{\mathbf{x}}\\ \ddot{\mathbf{x}}\\ \hline \dot{\mathbf{p}}_r\end{bmatrix} &= \mathbf{A}_c\mathbf{x}^+(t) + \mathbf{B}_c(\mathbf{f}_e(t) + \mathbf{u}(t))\\ \mathbf{y}(t) &= \mathbf{C}_c\mathbf{x}^+(t)\end{aligned} \tag{1}$$

where $\mathbf{u}$ is the 6DOF control force vector, $\mathbf{f}_e$ is the wave excitation force vector and the position and velocity state vector is given by $[\mathbf{x}\ \ \dot{\mathbf{x}}]^T$. The state vector is augmented with the auxiliary states $\mathbf{p}_r$ relating to a 4^{th} order State-Space approximation $\mathbf{G}_r$ of the radiation impulse response functions described by

$$\begin{aligned}\dot{\mathbf{p}}_r(t) &= \mathbf{A}_r\mathbf{p}_r(t) + \mathbf{B}_r\dot{\mathbf{x}}(t)\\ \textstyle\int_0^t \mathbf{K}_r(t-\tau)\dot{\mathbf{x}}(\tau)d\tau &\approx \mathbf{C}_r\mathbf{p}_r(t) + \mathbf{D}_r\dot{\mathbf{x}}(t)\end{aligned} \tag{2}$$

where the matrices $\{\mathbf{A}_r, \mathbf{B}_r, \mathbf{C}_r, \mathbf{D}_r\}$ describing $\mathbf{G}_r$ are computed using a standard BEM solver. Including all 36 modes in the state-space model results in 144 states.

The augmented plant and output matrices are obtained from linearising the WEC system about its nominal resting position, giving

$$\begin{aligned}\mathbf{A}_c &= \left[\begin{array}{cc|c}\mathbf{0}^{6\times6} & \mathbf{I}^{6\times6} & \mathbf{0}^{6\times144}\\ -\mathbf{M}_\infty^{-1}\mathbf{K}_0 & -\mathbf{M}_\infty^{-1}(\mathbf{B}_v+\mathbf{D}_r) & -\mathbf{M}_\infty^{-1}\mathbf{C}_r\\ \hline \mathbf{0}^{144\times6} & \mathbf{B}_r & \mathbf{A}_r\end{array}\right]\\ \mathbf{B}_c &= \left[\begin{array}{c}\mathbf{0}^{6\times6}\\ \mathbf{M}_\infty^{-1}\\ \hline \mathbf{0}^{144\times6}\end{array}\right] \quad \mathbf{C}_c = \left[\begin{array}{cc|c}\mathbf{0}^{6\times6} & \mathbf{I}^{6\times6} & \mathbf{0}^{6\times144}\end{array}\right]\end{aligned} \tag{3}$$

where $\mathbf{M}_\infty$ is the sum of the float mass matrix and infinite added mass matrix $\mathbf{A}_\infty$ which is obtained from the BEM solution, $\mathbf{K}_0$ is the linearised stiffness matrix (see Scruggs et al. (2013)) and $\mathbf{B}_v$ is a linear viscous damping matrix empirically tuned to experimental data (Faraggiana et al. (2019)). Following a model reduction process, the number of states can be reduced to 36, resulting in a model suitable for control system design.

The state-space model is then discretized using a first-order hold approximation, such that

$$\begin{aligned}\mathbf{x}_{k+1}^+ &= \mathbf{A}\mathbf{x}_k^+ + \mathbf{B}(\mathbf{f}_{ek} + \mathbf{u}_k)\\ \mathbf{y}_k &= \mathbf{C}\mathbf{x}_k^+\end{aligned} \tag{4}$$

4. MODEL PREDICTIVE CONTROL

The predicted state trajectory over the prediction horizon N is generated from the discrete time state-space model (4) according to

$$\mathbf{X}_k^+ = \boldsymbol{\mathcal{M}}\mathbf{x}_k^+ + \boldsymbol{\mathcal{C}}(\hat{\mathbf{F}}_{e|k} + \mathbf{U}_k) \tag{5}$$

where $\mathbf{U}_k$ and $\hat{\mathbf{F}}_{e|k}$ are the stacked future control force and estimated excitation force matrices given by

$$\mathbf{U}_k = \begin{bmatrix}\mathbf{u}_k\\ \mathbf{u}_{k+1}\\ \vdots\\ \mathbf{u}_{k+N-1}\end{bmatrix} \quad \hat{\mathbf{F}}_{e|k} = \begin{bmatrix}\hat{\mathbf{f}}_{e|k}\\ \hat{\mathbf{f}}_{e|k+1}\\ \vdots\\ \hat{\mathbf{f}}_{e|k+N-1}\end{bmatrix} \tag{6}$$

$$\boldsymbol{\mathcal{M}} = \begin{bmatrix}\mathbf{A}\\ \mathbf{A}^2\\ \vdots\\ \mathbf{A}^N\end{bmatrix} \quad \boldsymbol{\mathcal{C}} = \begin{bmatrix}\mathbf{B} & \mathbf{0} & \cdots\ \mathbf{0}\\ \mathbf{AB} & \mathbf{B} & \cdots\ \mathbf{0}\\ \vdots & \vdots & \ddots\\ \mathbf{A}^{N-1}\mathbf{B} & \mathbf{A}^{N-2}\mathbf{B} & \cdots\ \mathbf{B}\end{bmatrix} \tag{7}$$

The control objective is to maximise the average absorbed power $\bar{w}$ over the prediction horizon through appropriate manipulation of the control force $\mathbf{u}$. This objective can be

expressed as the following discrete integral (Soltani et al. (2014))

$$\bar{w} = \frac{1}{N}\sum_{i=k}^{k+N} \mathbf{x}_i^+ \mathbf{s}\mathbf{u}_i = \mathbf{X}^{+^T}\mathbf{S}\mathbf{U} \tag{8}$$

where $\mathbf{S}$ is the N-block-diagonal matrix of $\mathbf{s}$, and

$$\mathbf{s} = \left[\, \mathbf{0}^{6\times 6} \;\; \mathbf{I}^{6\times 6} \;\; \mathbf{0}^{24\times 6} \,\right]^T \tag{9}$$

Substituting the state prediction (5) into the objective function (8) gives the quadratic cost function

$$J(\mathbf{U}_k) = \mathbf{U}_k^T \mathbf{H}\mathbf{U}_k + \mathbf{F}^T\mathbf{U}_k \tag{10}$$

where $\mathbf{H} = \boldsymbol{\mathcal{C}}^T\mathbf{S}$, $\mathbf{F}^T = \mathbf{X}_k^{+T}\boldsymbol{\mathcal{M}}^T\mathbf{S} + \hat{\mathbf{F}}_{e|k}^T\boldsymbol{\mathcal{C}}^T\mathbf{S}$. Since $\mathbf{H}$ is time-invariant it is computed offline, while $\mathbf{F}^T$ is updated each time step according to the most recent estimates of the state prediction $\mathbf{X}_k^+$ and forecast excitation force $\hat{\mathbf{F}}_{e|k}$. To improve the tractability of the optimisation, the cost function is convexified with the addition of small diagonal terms to $\mathbf{H}$ equal to the absolute value of its smallest eigenvalue (Li and Belmont (2014)), such that $\hat{\mathbf{H}} = \mathbf{H} + |\lambda_{min}|(\mathbf{H})$.

With the addition of state constraints designed to limit surge and heave position amplitudes, the optimisation problem is defined as

$$\begin{aligned} &\underset{\mathbf{U}_k}{\text{maximise}} \;\; \mathbf{U}_k^T\hat{\mathbf{H}}\mathbf{U}_k + \mathbf{F}^T\mathbf{U}_k \\ &\text{subject to} \begin{bmatrix} \boldsymbol{\mathcal{C}}_i \\ -\boldsymbol{\mathcal{C}}_i \end{bmatrix} \mathbf{u}\,[k] \le \begin{bmatrix} \bar{\mathbf{x}} \\ -\underline{\mathbf{x}} \end{bmatrix} + \begin{bmatrix} -\mathbf{A}^i \\ \mathbf{A}^i \end{bmatrix}, \; i = 1:N \end{aligned} \tag{11}$$

where $\bar{\mathbf{x}}$ and $\underline{\mathbf{x}}$ are the upper and lower bounds of the state variables, respectively. Limits on control force are not imposed within the optimisation here. In part, this is to provide a fair comparison to benchmark data from the optimally tuned passive system which does not include these limits. There is a necessary constraint on control force to avoid slack PTO tethers, but including this in the optimisation can result in constraint conflict and subsequent intractability of the solution. Therefore this constraint is imposed as a dynamic saturation on the control force post optimisation, exactly as it is for the passive system.

Performing this optimisation and applying only the output for the next time step to the WEC results in a 6DOF control force in Cartesian space. This control force is distributed to the four PTO tethers according to

$$\mathbf{u}_{PTO} = \mathbf{J}_0^T\mathbf{u} \tag{12}$$

where $\mathbf{J}_0^{-1}$ is the inverse kinematic Jacobian matrix (see Hillis et al. (2019) for details).

5. WAVE EXCITATION FORCE ESTIMATION AND FORECASTING

The wave excitation or disturbance force is not measurable, but is a necessary input to the optimisation problem in order to generate the appropriate control force. In order to estimate the disturbance force it is required to know the dynamics of the float body and all other forces acting upon it, as well as estimates or measurements of the float motion. It this then possible to implement a dynamic observer to estimate the wave excitation force. Here we use a Kalman filter approach as described in Nguyen and Tona (2018) to achieve this. As we are able to measure the tether forces directly using load cells, we can directly measure the combination of control force and passive spring force.

The state vector $\mathbf{x}^+$ is further augmented with the estimated disturbance force $\hat{\mathbf{f}}_e$. Maintaining the notation $\mathbf{x}^+$ for the further augmented state vector for convenience, the discretized system dynamics are now described by

$$\begin{aligned} \mathbf{x}_{k+1}^+ &= \begin{bmatrix} \mathbf{x}^+ \\ \hat{\mathbf{f}}_e \end{bmatrix}_{k+1} = \mathbf{A}^+\mathbf{x}_k^+ + \mathbf{B}^+\left(\hat{\mathbf{f}}_e - \mathbf{f}_{PTO}\right)_k + \boldsymbol{\epsilon}_k \\ \mathbf{y} &= \mathbf{C}^+\mathbf{x}_k^+ + \boldsymbol{\mu}_k \end{aligned} \tag{13}$$

where $\boldsymbol{\epsilon}$ describes the random walk process for excitation force estimation and unmodelled dynamics, and $\boldsymbol{\mu}$ describes measurement noise. $\mathbf{f}_{PTO}$ is the Cartesian vector of tether tension forces, derived from direct measurement of the combined control and spring forces according to

$$\mathbf{f}_{PTO} = \mathbf{J}_0^{-T}(\mathbf{u}_{PTO} + \mathbf{K}_o\mathbf{x}) \tag{14}$$

where $\mathbf{J}_0^{-T}$ is the transpose of the inverse kinematic Jacobian matrix. The system matrices are defined as follows:

$$\mathbf{A}^+ = \begin{bmatrix} \mathbf{A} & \mathbf{B} \\ \mathbf{0} & \mathbf{I} \end{bmatrix} \quad \mathbf{B}^+ = \begin{bmatrix} \mathbf{B} \\ \mathbf{0} \end{bmatrix} \quad \mathbf{C}^+ = [\,\mathbf{C}\;\mathbf{0}\,] \tag{15}$$

A standard Kalman filter is then used to estimate $\mathbf{x}_{k+1}^+$.

The estimated wave excitation force must also be forecast over a prediction horizon for the MPC optimisation. In practice the choice of horizon must balance the improvement in power absorption from the optimisation against the quality of the estimated wave force which degrades as the forecast horizon increases. Inevitably there will be a point where the estimation is not accurate enough to yield power increases. A further limitation is the computational load, which increases as the prediction horizon increases but must be completed between computational steps. A number of methods for forecasting are studied in Fusco and Ringwood (2010). Based on this study an auto-regressive (AR) modelling technique is adopted here.

The N-step ahead prediction of the excitation force at instant k is given by

$$\hat{\mathbf{f}}_e\,[k+N|k] = \sum_{i=1}^{n} \hat{a}_i \hat{\mathbf{f}}_e\,[k+N-i|k] \tag{16}$$

where $\hat{a}_i$ are the AR coefficients resulting from an estimation procedure. Here we use the Burg method to estimate the AR parameters. The training data used for this estimation is excitation force data generated for sea states with the same spectra, but different random seeds (and hence different time-domain values in the sequences). An AR filter with order 200 was found to give reasonable results.

Figure 2 shows the goodness-of-fit for three irregular sea states with a range of prediction horizons. All spectra are Pierson-Moskowitz type with a range of energy periods and significant wave heights. We observe reasonable estimation with the quality reducing as the prediction horizon and energy period of the sea states increase. The time-domain plot of the "actual" excitation force (from WEC-Sim simulations) versus the 10s ahead predictions for the surge direction for the three sea states are shown in Figure 3 by way of example.

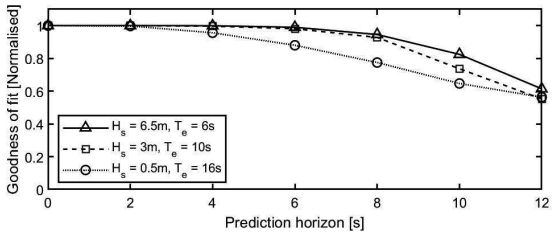

Fig. 2. Goodness of fit of wave excitation force predictions for a range of horizons and sea states

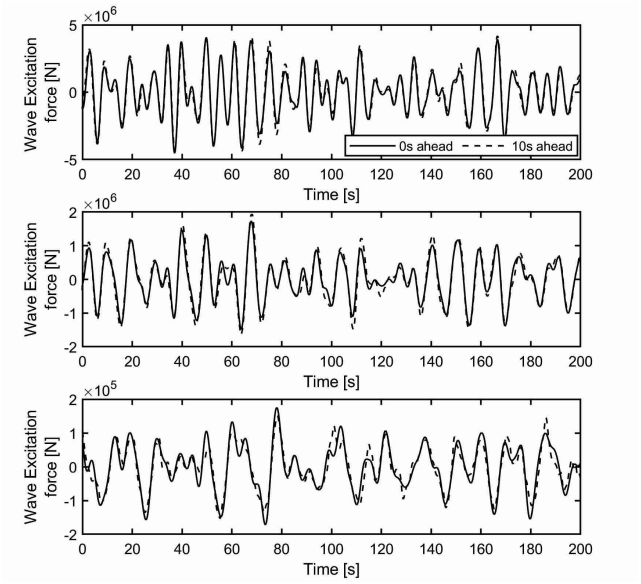

Fig. 3. Actual vs 10s ahead predictions of wave excitation forces. TOP: $H_s = 6.5$m, $T_e = 5$s, MIDDLE: $H_s = 3$m, $T_e = 10$s, BOTTOM: $H_s = 0.5$m, $T_e = 16$s

6. SIMULATION RESULTS: IDEALISED CASE

A simulation study was conducted whereby the system under control is an exact match for the state-space model embedded within the MPC optimisation. Many optimal control studies for WECs are limited to this ideal case. As a benchmark for performance comparison, a passively controlled system (i.e. the PTO forces are proportional to the PTO tether velocities) was tuned for each sea state. For this and all subsequent power plots, power values are normalised against the peak mean value achieved with the tuned passive system in the most energetic sea state.

The ideal system was then placed under MPC with both ideal prediction and real-time prediction scenarios with a range of prediction horizons. Figure 4 shows the results for mean power absorbed for each case. It is seen that a horizon of at least 5s is required to increase absorbed power compared to the optimal passive case in all three sea states. We also see the expected reduction in power as the horizon increases for the cases where online prediction is used. Again, as expected this effect is most pronounced for the sea state with the highest energy period as this case has the least accurate forecasting. Based on this and the fact that beyond a 10s horizon the benefits drop off, a pragmatic horizon to use would seem to be 10s, which is in line with other studies. Figure 5 shows the instantaneous absorbed mechanical power for the three sea states using a 10s horizon. The mean power gains for MPC with online prediction compared to the tuned passive system are rather dramatic, being up to a factor of 2.5. The reduction in mean power absorption as a result of using online prediction rather than assuming perfect future knowledge with MPC is relatively minor, being 15% in the worst case.

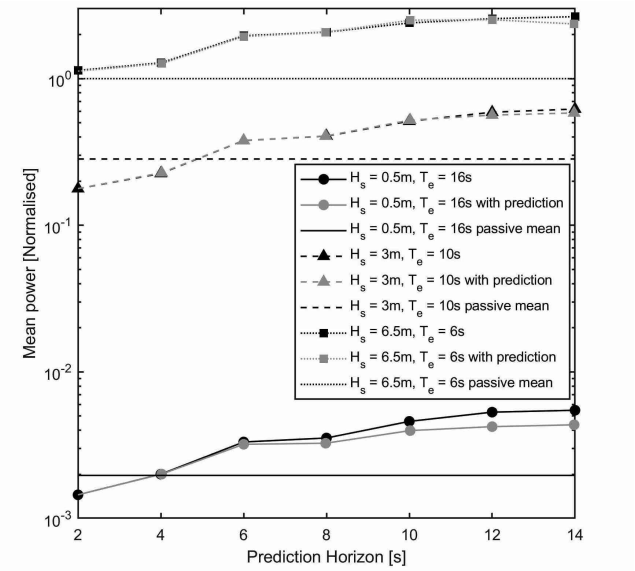

Fig. 4. Mean power absorbed for different horizons with and without online prediction of excitation force for idealised system

7. SIMULATION RESULTS - WEC-SIM

The MPC constrained optimisation together with estimation and 10s ahead prediction of the excitation force is now applied to a nonlinear WEC-Sim model of the multi-DOF WEC (see Figure 1 for an image of the simplified system geometry). These simulations, therefore, represent a more realistic scenario as the controller is deployable in a real system and there is model mismatch between the state-space idealisation embedded within the optimisation and the actual system under control. The float and reactor are connected with four taut PTO tether lines, each modelled as a translational PTO actuation force incorporating a spring stiffness and damping force, a universal joint and gimbal. All motions and forces are available for use by the control strategy within this model and the control force applied to each PTO is incorporated by adding to the external preload force on each PTO. The damping force is used only for the benchmark passive optimally

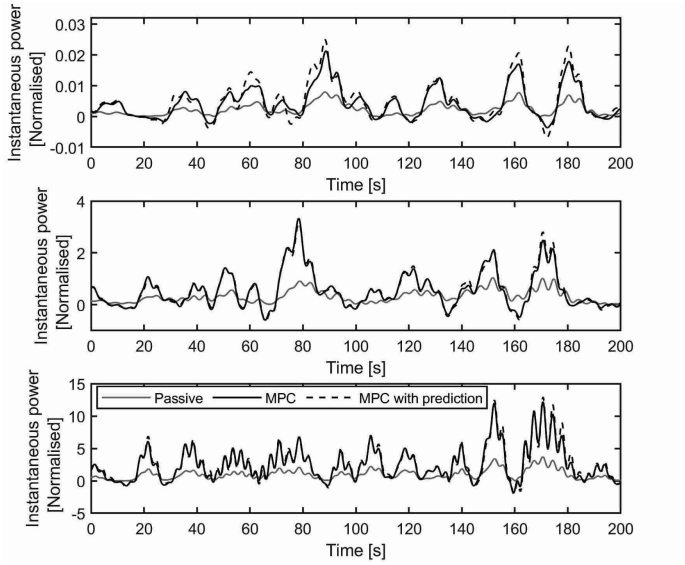

Fig. 5. Instantaneous absorbed power in irregular sea states for passive and MPC systems with and without prediction using idealised system with a 10s horizon

tuned system and is set to zero for active control. Irregular waves are applied in the x-direction.

Figure 6 shows the surge (x), heave (z) and pitch (rotation about y) displacement responses of the float in the most energetic sea state ($H_s = 6.5$m, $T_e = 6$s). Results are presented only for this sea state for the sake of brevity and because it shows the most interesting results as all constraints are active. We observe that the controlled motions are significantly exaggerated compared to the optimal passive system as we would expect. We also see that the heave position limit is not in danger of being exceeded while the surge position limit is largely adhered to, though not in a hard sense.

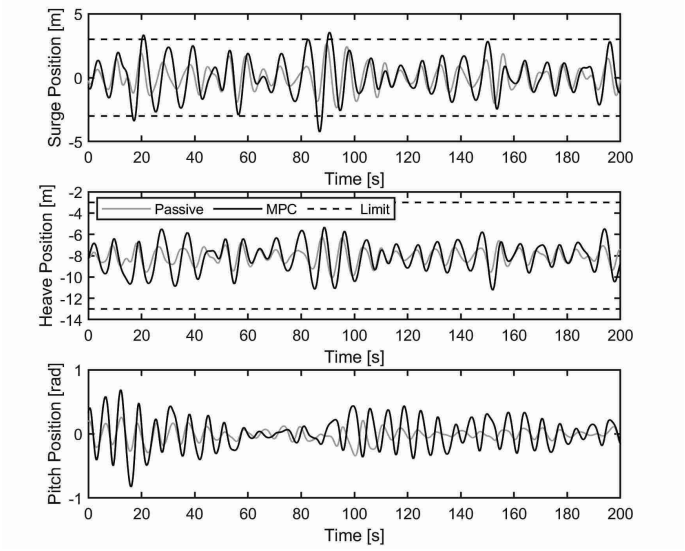

Fig. 6. Surge, heave and pitch displacement responses of the float in Pierson-Moskowitz sea state ($H_s = 6.5$m, $T_e = 6$s). Results shown for passive system and MPC with 10s horizon

The explanation of this comes from studying the accompanying Figure 7 which shows the PTO control forces and line tensions. It is observed that the dynamic limit applied to avoid PTO tether slackness is active at the times when the surge position limit is exceeded. This could potentially be avoided by incorporating the slack tether constraint into the MPC optimisation. However, as previously stated, this could cause problems with solution feasibility. The way to solve this would be to incorporate slack variables to the position constraint, but this would result in similar behaviour in terms of limit violation. Figure 8 shows the instantaneous absorbed mechanical

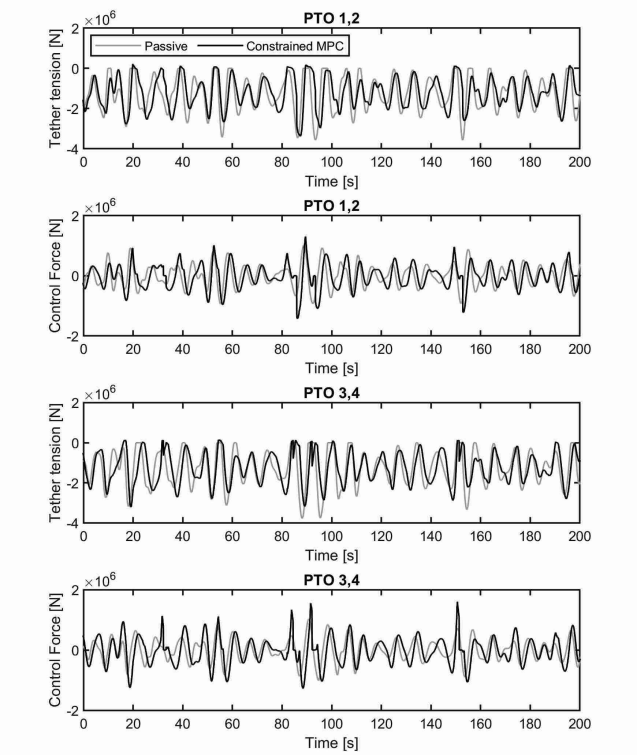

Fig. 7. PTO forces and tether tensions in Pierson-Moskowitz sea state ($H_s = 6.5$m, $T_e = 6$s) for passive system and MPC with 10s horizon

power for each sea state with the passive and constrained MPC solutions. We see that large increases in power are seen for the lowest energy sea state ($H_s = 0.5$m, $T_e = 16$s), though not as impressive as seen for the same case with an idealised system (see Figure 5). The mean power increase here is +68%. The 10s sea state shows a mean power increase of +27% - again far below that suggested by the idealised simulations. The highest energy sea state results in a reduction of absorbed power compared to the passive system of -3%. These results are summarised against those for the idealised system in table 1.

Table 1. Mean power increases compared to tuned passive system

Sea State		Mean power increase	
T_e[s]	H_s[m]	Idealised model	WEC-Sim model
16	0.5	+100%	+68%
10	3.0	+81%	+27%
6	6.5	+150%	−3%

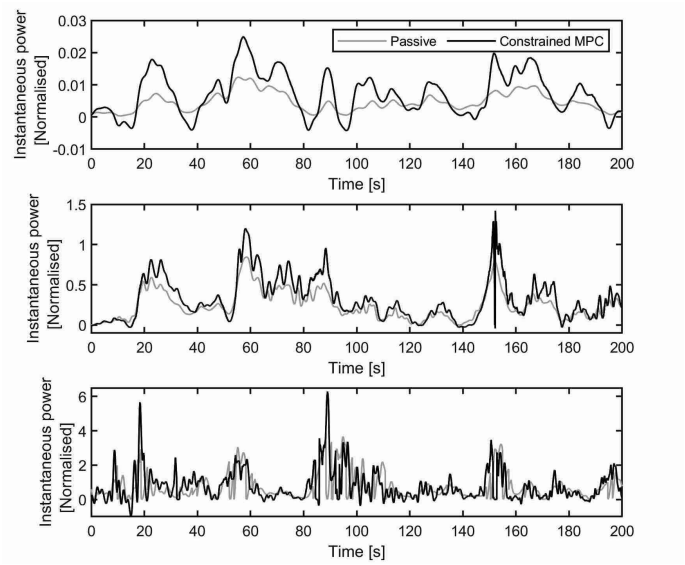

Fig. 8. Instantaneous absorbed power in irregular sea states for passive and MPC systems with prediction a 10s horizon using WEC-Sim model

8. CONCLUSIONS

An MPC law has been applied to the multi-DOF WaveSub WEC in idealised and more realistic scenarios with the purpose of investigating the effects of modelling and excitation force prediction errors on system performance. The results show that prediction errors have a relatively minor effect on power absorption, though this is dependent on the quality of the prediction. This study considers only a small range of sea states and real sea states may occur which are less predictable. Model mismatch is a significant issue and results in a very large reduction in power absorption compared to the ideal case. In part this is due to changes in the controlled system stiffness matrix as the float moves away from its nominal position, and in part because the kinematic Jacobian matrix used to distribute the control forces to the PTO tethers also changes. This could potentially be alleviated by employing a nonlinear MPC law such as in Richter et al. (2013), however the already considerable computational burden would further increase along with the risk of infeasibility in the optimisation.

This study, though a step beyond using an idealised state-space model as the target system, is still limited by having at its heart the linearised BEM hydrodynamic coefficients comprising part of the system dynamics. In reality these coefficients will be nonlinear for large motions and complex geometries. Other studies e.g. Ringwood et al. (2019) have shown the sensitivity of system performance to these inaccuracies. The performance results achieved here suggest that significant improvements can still be achieved with an MPC law in spite of these errors. Significant power gains over the optimised passive system were achieved in the more commonly occurring lower energy sea states. However, it is arguably better in reality to use a control strategy that is inherently more robust to uncertainty e.g. the relatively recently proposed pseudo-spectral optimal strategy, see Bacelli and Ringwood (2015) or an AVT strategy as noted in Ringwood et al. (2019).

REFERENCES

Bacelli, G. and Ringwood, J. (2015). Numerical optimal control of wave energy converters. *IEEE Transactions on Sustainable Energy*, 6.

Cretel, J., Lightbody, G., Thomas, G., and Lewis, A. (2011). Maximisation of energy capture by a wave-energy point absorber using model predictive control. In *Proceedings of the 18th IFAC World Congress*. Milan, Italy.

Faraggiana, E., Whitlam, C., Chapman, J., Hillis, A., Roesner, J., Hann, M., Greaves, D., Yu, Y.H., Ruehl, K., Masters, I., Foster, G., and Stockman, G. (2019). Computational modelling and experimental tank testing of the multi float wavesub under regular wave forcing. *under review with Renewable Energy*.

Fusco, F. and Ringwood, J.V. (2010). Short-term wave forecasting for real-time control of wave energy converters. *IEEE Transactions on Sustainable Energy*, 1, 99–106.

Hals, J., Falnes, J., and Moan, T. (2010). Constrained optimal control of a heaving buoy wave-energy converter. *Journal of Offshore Mechanics and Arctic Engineering*, 133(1), 011401–011401.

Hillis, A., Whitlam, C., Brask, A., Chapman, J., and Plummer, A. (2019). Power capture gains for the wavesub submerged wec using active control. In D. Vicinanza (ed.), *Proceedings of the Thirteenth European Wave and Tidal Energy Conference*. EWTEC, Naples, Italy.

Li, G. and Belmont, M.R. (2014). Model predictive control of a sea wave energy converter: a convex approach. *IFAC Proceedings Volumes*, 47(3), 11987 – 11992. 19th IFAC World Congress.

Nguyen, H.N. and Tona, P. (2018). Wave excitation force estimation for wave energy converters of the point-absorber type. *IEEE Transactions on Control Systems Technology*, 26(6), 2173–2181.

O'Sullivan, A. (2017). Power maximisation of a wave energy converter using predictive control: Robustness to system mismatch. In A. Lewis (ed.), *Proceedings of the Twelfth European Wave and Tidal Energy Conference*. EWTEC, Cork, Ireland.

Richter, M., Magana, M.E., Sawodny, O., and Brekken, T.K.A. (2013). Nonlinear model predictive control of a point absorber wave energy converter. *IEEE Transactions on Sustainable Energy*, 4(1), 118–126.

Ringwood, J.V., Mérigaud, A., Faedo, N., and Fusco, F. (2019). An analytical and numerical sensitivity and robustness analysis of wave energy control systems. *IEEE Transactions on Control Systems Technology*, 1–12.

Scruggs, J., Lattanzio, S., Taflanidis, A., and Cassidy, I. (2013). Optimal causal control of a wave energy converter in a random sea. *Applied Ocean Research*, 42, 1 – 15.

Soltani, M.N., Sichani, M.T., and Mirzaei, M. (2014). Model predictive control of buoy type wave energy converter. *IFAC Proceedings Volumes*, 47(3), 11159 – 11164. 19th IFAC World Congress.

Yu, Y., Lawson, M., Ruehl, K., and Michelen, C. (2014). Development and demonstration of the wec-sim wave energy converter simulation tool. In *Proceedings of the 2nd Marine Energy Technology Symposium, Seattle, WA*.